Plate mode identification using modal analysis based on microphone array measurements

A.L. van Velsen, E.M.T. Moers, I. Lopez Arteaga, H. Nijmeijer
Department mechanical engineering, Eindhoven University of Technology, Eindhoven, The Netherlands.

Summary
The goal of this study is to investigate the possibilities of identifying the modal properties of plate-like structures by applying modal analysis on acoustic pressure measurements using a microphone array. Since this is a contact-less measurement method, the dynamic response of the system is not affected by the measurement. The modal properties are determined by using the rational fraction polynomial method (RFP), which is an indirect frequency domain modal analysis method. Two measurement techniques are compared; (1) measurements with accelerometers and (2) with a microphone array. Using planar near-field acoustic holography (PNAH), the displacement field of the vibrating source is calculated from the pressure data captured with the microphone array. The receptance frequency response functions are determined from the displacement field. The measurements are performed on a free plate. The pressure is captured in the near-field of the plate. The aperture of the microphone array is larger than the plate dimensions. The frequency domain of interest is 0 - 1500 Hz which contains the first four resonance frequencies of the plate. Modal analysis based on acceleration measurements give good results, all modal properties are obtained very well. The eigenfrequencies resulting from the modal analysis based on PNAH are comparable to the eigenfrequencies obtained using the accelerometers. The mode shapes are clearly visible in the from the acoustic pressure reconstructed displacement field. However, the mode shapes identified by modal analysis are not accurate. A possible reason is the limited quality of the reconstruction of the drive point frequency response function.

PACS no. 43.60.Fg, 43.60.Sx

1. Introduction

Unwanted vibrations cause, among others, noise and wear. These vibrations can be captured in a modal model which describes the dynamic response of the system. This modal model can be used to control the vibrations, design structures, evaluate dynamics, develop experimental based models, et cetera. The modal properties of a structure are needed to compose its modal model. In this paper the possibilities of identifying the modal properties of plate-like structures by applying modal analysis on acoustic pressure measurements using a microphone array and planar near-field acoustic holography (PNAH) is investigated.

PNAH is a method to localize sound sources [1]. Pressure is measured in the near-field of the expected source. This is done with a microphone array which contains a high number of microphones. The acoustic information at the sensor plane is typically transformed to acoustic vibration or other acoustic quantities to a location near or on the source. This transformation is performed in the wave number domain by solving an inverse problem. This problem is ill-posed due to the existence of decaying, evanescent waves. Regularization is used to overcome this problem [2].

The measurements are contact-less which makes it interesting to use for identification purposes. Prezelj *et al.* identified the mode shapes of a completely free plate [3]. It is shown that the reconstructed source velocity field from the acoustic pressure measurements is different to the velocity field when measured directly. The amplitude of the acoustic pressure and the reconstructed velocity field is low at the edges due to a short-circuit effect. A similar result is shown by J.L. Potter *et al.* [4]. In this work, modal analysis is performed on measurement data obtained from a microphone array and compared with measurement data from a laser vibrometer.

In this paper, the normal plate velocity is retrieved by Fourier based PNAH. The result of frequency response functions (FRFs) and the modal analysis are compared with those obtained with accelerometers.

The analysis is applied to a completely free rectangular plate, which mode shapes and eigenfrequencies are described by A.W. Leissa [5, p. 87].

2. Modal analysis method

The response of a structure to a point force can be described by modal superposition [6]. Consider a plate with mode shapes $\phi_r(x,y)$ for the corresponding angular eigenfrequencies ω_r. Assume viscous damping with the resulting modal damping ratios ζ_r, then the transverse displacement η is given by:

$$\eta(x,y,t) = \sum_{r=1}^{\infty} \frac{\tilde{F}}{M_r} \frac{\phi_r(x,y)\phi_r(x_f,y_f)}{\omega_r^2 - \omega^2 + 2i\zeta_r\omega_r\omega} e^{i\omega t}, \quad (1)$$

for a harmonic force with amplitude $\tilde{F}$ at position (x_f, y_f), generalized mass M_r and angular frequency ω for all modes r. Modal analysis is used to find the modal properties (ϕ_r, ω_r, ζ_r) in the modal model given in (1). This is done by fitting frequency response functions (FRFs) obtained with modal testing. Since the result of PNAH is in the frequency domain a frequency domain method is used. In this study the rational fraction polynomial method (RFP) is used, which is a multiple-degree of freedom method. This method makes use of complex orthogonal polynomials to fit the partial fraction form of the receptance FRF [7]:

$$\alpha(\omega) = \sum_{r=1}^{N} \frac{A_r + i\omega B_r}{\omega_r^2 - \omega^2 + i2\zeta_r\omega_r\omega}, \quad (2)$$

where A_r and B_r are the modal constants, ω_r is the frequency of mode r, ζ_r is the damping ratio of mode r and N is the total number of modes included in the model. This partial fraction form can also be expressed in terms of the ratio between two complex orthogonal polynomials φ and θ:

$$\alpha(\omega) = \frac{\sum_{k=0}^{2N-1} c_k\varphi_k}{\sum_{k=0}^{2N} d_k\theta_k}, \quad (3)$$

with c_k and d_k the polynomial coefficients [6].

The coefficients are obtained by minimizing a difference function. The error is defined as the difference between the fit, $\alpha(\omega)$, and the measurement data, $\tilde{\alpha}(\omega)$, which is minimized for each frequency ω_l

$$e_l = \alpha(\omega_l) - \tilde{\alpha}(\omega_l) = \frac{\sum_{k=0}^{2N-1} c_k\varphi_{l,k}^{+}}{\sum_{k=0}^{2N} d_k\theta_{l,k}^{+}} - \tilde{\alpha}(\omega_l). \quad (4)$$

The difference function e_l is not linear in its unknown parameters. To get a linear system of equations, the function e_l is modified by multiplying with the denominator term $\sum_{k=0}^{2N} d_k\theta_{i,k}^{+}$ and by making last coefficient of denominator polynomial equal to one, $d_{2N} = 1$

$$\begin{aligned} e_l\prime &= e_l \sum_{k=0}^{2N} d_k\theta_{i,k}^{+} \\ &= \sum_{k=0}^{2N-1} c_k\varphi_{l,k}^{+} - \tilde{\alpha}(\omega_l)\left(\sum_{k=0}^{2N-1} d_k\theta_{l,k}^{+} + \theta_{l,2N}^{+}\right). \end{aligned} \quad (5)$$

2.1. Modal property extraction

To find the modal properties, the fitted polynomials in terms of complex othogonal polynomials, as in (3), are transformed into ordinary polynomials, which results in (6):

$$\alpha(\omega) = \frac{\sum_{k=0}^{2N-1} a_k(i\omega)^k}{\sum_{k=0}^{2N} b_k(i\omega)^k}. \quad (6)$$

This transformation is described in [6, p. 245]. The problem is not directly solved for ordinary polynomials, because the orthogonal properties of the orthogonal polynomials are used to simplify the problem, [6]. After the transformation, the modal properties of the system can be found by writing the system in the partial fraction form:

$$\alpha(\omega) = \sum_{k=0}^{2N} \frac{z_k}{i\omega - p_k}, \quad (7)$$

in which the poles, p_k, follow from the roots of the denominator polynomial of (6), and in which z_k are the residues.

2.1.1. Eigenfrequencies and damping ratios

Combining (6) and (2), it can be found that the poles equal $p_k = -\omega_r\zeta_r + i\omega_r\sqrt{1-\zeta_r^2}$. Thus the eigenfrequency equals $\omega_r = |p_r|$ and the damping ratio equals $\zeta_r = -\frac{|p_r|}{\mathrm{Re}(p_r)}$ [8].

2.1.2. Mode shapes

The modal constants or mode shapes follow from writing each FRF in the partial fraction form, as given in (2). From which ${}_rC_{jk} = A_r + i\omega B_r$ can be found, which is the modal constant for mode r measured at position j with an excitation at position k. This modal constant is the numerator term of (7). The modal constant can also be written in terms of mode shapes: ${}_rC_{jk} = \phi_{jr}\phi_{kr}$. In which ${}_rC_{jk}$ is the modal constant for mode r measured at position j with an excitation at position k. Thus, at a drive point measurement, the modal constant equals ${}_rC_{kk} = \phi_{kr}\phi_{kr}$. Which means that the mode shape element of the column corresponding to the mode shape of mode r at each response point can only be retrieved when the set of measurements contains a drive-point measurement

$$\phi_{kr} = \sqrt{{}_rC_{kk}} \tag{8}$$

$$\phi_{jr} = \frac{{}_rC_{jk}}{\phi_{kr}} \tag{9}$$

Combining the modal constants for one mode of all response points, results in the mode shape of mode r.

Since the eigenfrequencies and the damping ratios are global properties, these should be constant for a structure. When multiple FRFs measured from one structure are fitted, the obtained eigenfrequencies and damping ratios can be averaged to find the global values. The mode shapes are local properties.

3. Planar near-field acoustic holography

Using the Fourier based method, PNAH, it is possible to find the relationship between the acoustic pressure in a plane at a certain distance and the velocity at the source plane $p(x, y, z_h) \Rightarrow \dot{\eta}(x, y, z_s)$:

$$\dot{\eta}(x, y, z_s) = \mathcal{F}_x^{-1}\mathcal{F}_y^{-1}\left[\mathcal{F}_x\mathcal{F}_y[p(x, y, z_h)]\frac{k_z}{\rho_0 ck}e^{jk_z(z_s-z_h)}\right], \tag{10}$$

where $\mathcal{F}_x$ is the spatial Fourier transform and $\mathcal{F}_x^{-1}$ is its inverse, k_z is the z-component of the wavenumber of the acoustic wave, ρ_0 and c are the mass density and the speed of sound respectively of the medium around the structure, in this study air is used.

When $z_h > z_s$ the source velocity field is obtained by solving an inverse problem, this method is called PNAH. In practical measurement situations additional preconditioning is required to optimize the discretization in (10). This includes an extrapolation in the $(x - y)$ directions of the microphone data to larger aperture and applying a spatial window. Further regularization in wavenumber domain is applied to overcome blow-up of noise in the inverse propagation step [2]. The steps to find the particle velocity in the source plane are: (1) measure the acoustic pressure, (2) calculate the spatial-frequency spectrum, (3) calculate wavenumber-frequency spectrum, (4) calculate and apply the velocity propagator, $G(k_x, k_y, z_s - z_h) = \frac{k_z}{\rho_0 ck}e^{jk_z(z_s-z_h)}$ and (5) determine spatial velocity field $\dot{\eta}$. For more details about the implementation see [9].

4. Measurements

To identify a structure, receptance FRFs are measured. An impact is applied and the response is measured with two separate types of sensors: (1) using accelerometers and (2) using a microphone array. The two procedures are shown schematically in Figure 1.

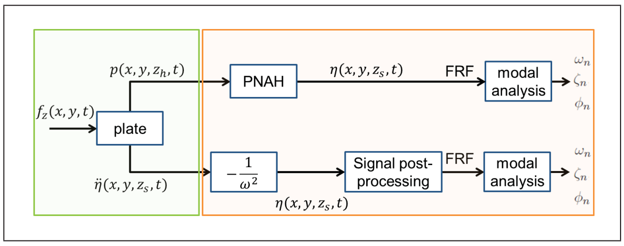

Figure 1. Overview of the measurements (green) and processing (red). Plate excited by force in the z-direction, f_z. Pressure, p, measured with microphone array at z_h and acceleration, $\ddot{\eta}$, measured at position z_s. Using PNAH the velocity field at the source, z_s, is reconstructed. Using modal analysis the modal properties are substracted from the FRFs.

4.1. Measurement setup

The measurements are performed on a rectangular aluminum plate with dimensions $300 \times 200 \times 10$ mm. The plate is supported in a frame with cord at the top corners to achieve free boundary conditions. The plate is excited with an impact hammer and the response is measured with accelerometers or with a microphone array. The accelerometers measure the acceleration direct on the plate, while the microphone array measures the acoustic pressure at a distance of 30 mm from the plate. Three accelerometers are moved to measure at 18 positions, including the drive point. The array consists of 1024 MEMS microphones (32×32), with a spacing of 20 mm and has a total measurement surface of 640×640 mm. The microphones are aligned with the accelerometer positions.

4.2. Data acquisition and signal processing

The acceleration measurements are performed with a Siglab data acquisition system. A bandwidth of 2000 Hz, a sampling frequency of 5120 Hz and a measurement time of 1.6 seconds is used. The measurements are windowed: a rectangular window is used for the force signal and an exponential window for the acceleration response signal. A total of 12 sets is measured from which the receptance FRFs are determined and finally averaged.

The measurements with microphones are performed using the array in combination with the Sorama DAQ which has a sampling frequency of $f_s = 46875$ Hz. A total of two seconds is captured, afterwards the data is manually triggered. This results in a measurement time of 1.16 seconds. The time signals from the array are windowed with a Hanning window. The force signal is windowed with a rectangular window. After windowing and calculating the frequency spectrum the pressure field is border padded, [10] using linear

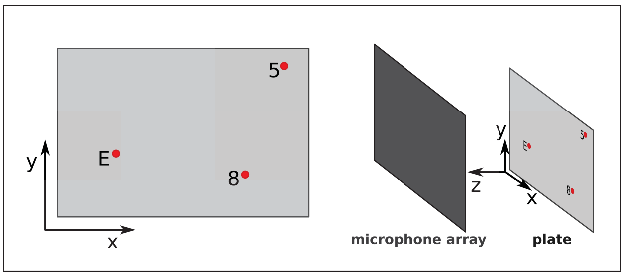

Figure 2. The plate with the three positions which are analyzed here: drive point (E), sensor (5) near edge, sensor (8) near center. At the right the orientation of the microphone array with respect to the plate is indicated.

Table I. Location resonant peaks for both measurement methods and the analytic eigenfrequencies [11].

n	Blevins	Acc. f_n [Hz]	Mics. f_n [Hz]
1	570	518	519
2	598	579	580
3	1291	1193	1203
4	1392	1356	1358

predictive border padding and a modified exponential wave number domain filter is applied, as described in [9]. To simplify processing it is chosen to take the filter cut-off wave number k_{co} constant over the frequency range of interest: $k_{co} = 45$ rad/s and a slope of 0.1. Then, using PNAH the receptance FRFs are calculated. A total of 9 data sets are gathered and averaged and a frequency range of 350-1500 Hz is analyzed.

5. Analysis of the results

From the acceleration measurements, the FRFs can be determined directly. While, from the acoustic pressure measurements, the FRFs follow from an additional step: PNAH as explained in section 3.

5.1. Analysis and comparison of modal testing results

The receptance FRFs are determined for all acceleration positions and the microphones corresponding to these positions. To illustrate the difference in data quality, three FRFs are shown in Figure 3 for both measurement methods. It contains the drive point, a position near the edge and near the center. These positions are indicated in Figure 2.

The resonance peaks can be compared using figure 2. The frequency of the resonant peaks and the theoretical values are shown in Table I. The resonance peaks are located at similar frequencies for both sets of FRFs. The peaks, however, differ from the analytic eigenfrequencies of Blevins [11], this can be caused by the fact that the plate is not perfectly cut and that the material properties are different.

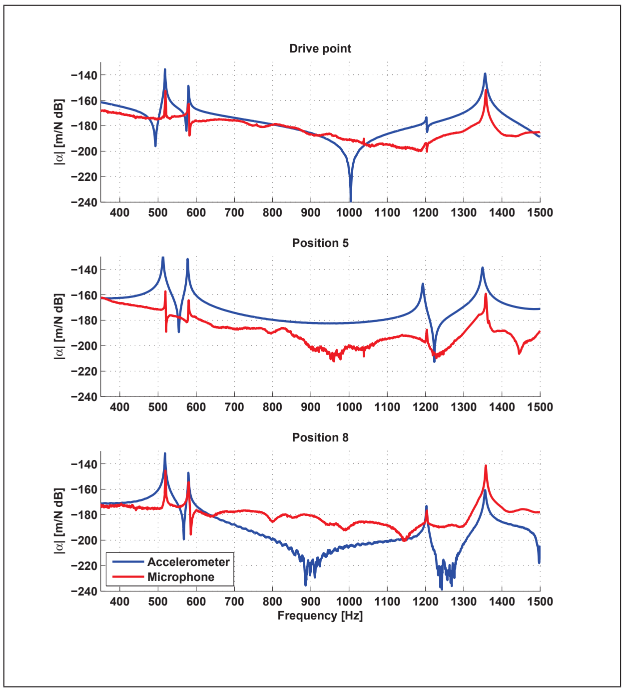

Figure 3. The receptance FRFs for three different sensor positions compared for both measurement methods. From top to bottom: Drive point (E), sensor (5) near edge, sensor (8) near center.

A microphone positioned above a source does measure the contribution of vibrations of the plate around this point. This could explain why the anti-resonances are not reconstructed as good as in the FRFs of the acceleration measurements. Especially the anti resonance between the second and the third mode is missing in the microphone data. Small differences in anti resonances were expected due to possible misalignment errors between the array and the sensor positions on the plate. Furthermore, low vibrations are difficult to measure because the radiated acoustic pressure drops below the signal to noise ratio.

The overall amplitude of the drive-point FRF and of the FRF from sensor position 8 are similar for both measurement methods. A difference can be seen for sensor position 5. The amplitude of the microphone FRFs is lower for the whole frequency domain. This can be explained by the distance to the edge of sensor position 5, which is only 20 mm. The amplitude of the pressure is low at the edges due to a short-circuit effect. This effect was also shown by [4, 3]. Furthermore, the amplitude of the FRFs are influenced by the filters applied in PNAH.

The FRFs of the remaining 15 positions are not shown in this paper. Similar remarks hold for these concerning their location and quality of FRF.

5.2. Analysis and comparison of modal analysis results

The obtained FRFs are fitted using the RFP method. The used modal analysis inputs are shown in Table

Table II. In this table all inputs for the modal analysis applied to the measurements on the plate are summed. With N the number of modes fitted, $[f_{min}\text{-}f_{max}]$ Hz the frequency domain of the fit and the mode numbers that are fitted.

	Acceleration measurements		
N	f_{min}	f_{max}	fitted modes
8	347	1437	1 – 4
	Microphone measurements		
N	f_{min}	f_{max}	modes
1	484	555	1
3	555	618	2
1	1156	1246	3
1	1246	1425	4

II. The first four modes of the acceleration measurements are fitted at once. The microphone measurements are fitted separately because this gave better results which might be caused by that the FRFs do not contain anti-resonances. The output of RFP method are the averaged N eigenfrequencies and damping ratios, and $18\times N$ modal amplitudes. The maximum fitting error (RMS error) of all measurements is in the order of 10^{-8} m/N.

5.2.1. Eigenfrequencies and damping ratios

The obtained (global) eigenfrequencies and damping ratios and the standard deviations are listed in Table III. The eigenfrequencies from the accelerometers have a high accuracy (standard deviation of $\sigma < 0.2\%$) for all modes. The fit of the microphone measurements is less accurate for the first two modes ($\sigma_1 = 2.7\%$ and $\sigma_2 = 1.2\%$). The third and fourth mode have also a high accuracy ($\sigma < 0.2\%$). The difference can be explained by the difference between the FRFs obtained for both methods. Besides, the accuracy might also differ since the modes are fitted in two different ways. Furthermore, the fourth and the third mode are above the coincidence frequency of the plate which means that these modes are expected to radiate more efficiently. The reconstruction of the velocity field is more accurate which will give better FRFs for the frequency domain above coincidence.

Almost all obtained damping constants have a standard deviation which is higher then the damping ratio itself or are negative. These damping ratios are thus inaccurate due to the large variation between the damping ratio before averaging to find the global damping ratios. The authors do not have an explanation for these large deviations. The fit error of the RFP method, as in (5), is weighted by the denominator of the FRF. The data away from the resonances is weighted more than at the resonances [12]. This might be an explanation for the poor reconstruction of the damping ratios.

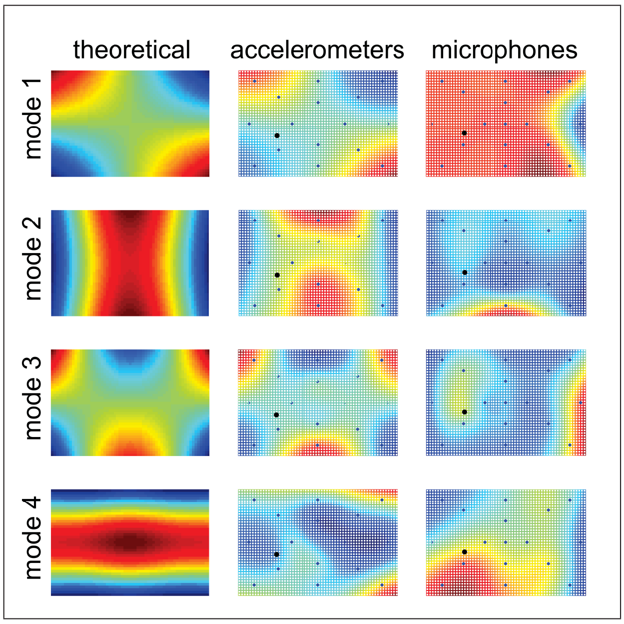

Figure 4. Mode shapes obtained using modal analysis for both measurement methods. The first column shows the analytic mode shapes of the first four modes, the second and third column are the mode shapes from the acceleration and the microphone measurements respectively. The drive point is indicated with a larger black dot.

5.2.2. Mode shapes

The obtained mode shapes are shown in Figure 4. The blue dots are the sensor positions. Between these points, the mode shape is interpolated using a thin plate spline interpolation method [13]. The mode shapes obtained from the acceleration measurements agree with the analytic mode shapes.

The velocity reconstructions, from the microphone measurements, at the resonances show the expected mode shapes clearly, see Figure 5. However, at the edges the amplitude is reduced. This will influence the modal analysis results. The drive-point FRF is of high influence on the mode shapes. A drive point FRF should contain all modes. Also, it is important that this FRF is of high accuracy because of its influence on the total mode shape, as indicated in (9). As it can be seen in Figure 3, the drive point FRFs does not have an anti-resonance after each peak. The found modal constants and the mode shapes calculated from the array measurements are not correct, as can be seen in the third column of Figure 4. The found mode shapes are not comparable to the mode shapes which are visible in the velocity reconstruction. The mode shapes found using modal analysis based on microphone measurements are not correct while the shapes were visible in the velocity field reconstructions and the mode shapes determined using modal analysis based on acceleration measurements have small differences with the analytic mode shapes.

Table III. Modal analysis results for both measurement methods: eigenfrequencies f_n [Hz] and damping ratios ζ_n [-] with standard deviation σ.

	Accelerometers				Microphones			
mode	f_n [Hz]	σ [Hz]	ζ_n [-]	σ [-]	f_n [Hz]	σ [Hz]	ζ_n [-]	σ [-]
1	519	0.23	0.0022	0.0077	516	13.9	-0.0075	0.0257
2	578	0.90	0.0010	0.0001	582	6.9	-0.0081	0.0341
3	1198	5.4	-0.0060	0.0072	1202	2.8	0.0005	0.0125
4	1320	5.5	0.0330	0.0836	1358	0.4	0.0002	0.0004

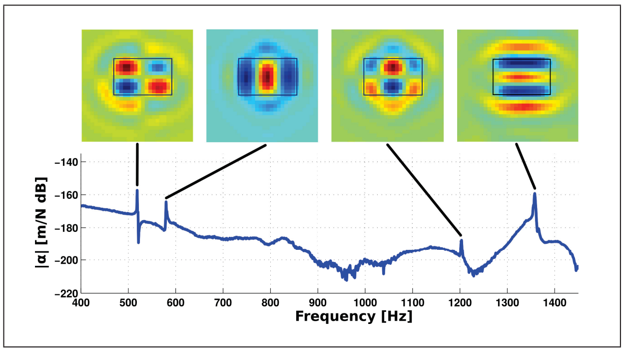

Figure 5. The reconstructions of the velocity field at the resonances, the mode shapes are clearly visible. The shown FRF is from sensor position 5.

6. CONCLUSIONS

The obtained frequency response functions based on accelerometer data and using PNAH on the pressure field reconstructed velocity are compared. The same resonance frequencies are found. However, since the microphone array measures the plate vibration indirectly and low vibrations are difficult to measure because the radiated acoustic pressure drops below the noise floor of the array, the anti-resonances are not observed as clearly as in the FRFs of the acceleration measurements. Furthermore, the FRFs resulting from the microphones at the edge of the plate have a lower amplitude than the FRF based on acceleration at the same location. This can be explained by hydrodynamical short-circuit.

For both methods, the modal analysis using the RFP method resulted in accurate identification of the eigenfrequencies. The obtained damping ratios are not accurate, the standard deviation is for some modes above 100%. The mode shapes identified from the acceleration measurements agreed with the analytic mode shapes. Although, at resonance frequencies the mode shapes can be clearly recognized in the with PNAH reconstructed displacement field, the obtained mode shapes are not comparable to the analytical mode shapes.

Based on the measurements and the comparison of the two methods it can be concluded that by applying modal analysis on acoustic pressure measurements for the low frequency domain the eigenfrequencies of a plate-like structure can be identified with a high accuracy. Identification of the mode shapes and the damping constants are shown not to be accurate. Further research is needed to investigate the influence of a different damping model or modal analysis method to improve the identifying the modal properties of plate-like structures using a PNAH based velocity reconstruction.

References

[1] E. G. Williams: Fourier Acoustics, Sound Radiation and Near-field Acoustical Holography. Academic Press, London, 1999.

[2] E. G. Williams: Regularization methods for near-field acoustical holography. The Journal of the Acoustical Society of America (2001), 1976-1988.

[3] J. Prezelj et al.: On acoustic very near field measurements. Mechanical systems and signal processing 40.1 (2013), 194-207.

[4] J. L. Potter et al.: Comparison of Modal Analysis Between Laser Vibrometry and NAH Measurements. Topics in Modal Analysis I, Volume 5. Springer New York, 2012, 471-480.

[5] A. W. Leissa: Vibration of plates. National Aeronautics and Space Administration, 1969.

[6] N. M. M. Maia et al.: Theoretical and Experimental Modal Analysis. Research Studies Press Taunton, 1997.

[7] M.H. Richardson and D.L. Formenti: Parameter estimation from frequency response measurements using rational fraction polynomials. Proc. IMAC 1982, 167-182.

[8] D.J. Ewins: Modal Testing: Theory, Practice, and Application. Research Studies Press LTD., Baldock, Hertfordshire, England, 2000.

[9] R. Scholte: Wavenumber domain regularization for near-field acoustic holography by means of modified filter functions and cut-off and slope iteration. ACTA Acustica united with Acustica 94.3, 2008, 339-348.

[10] R. Scholte, et al.: Truncated aperture extrapolation for Fourier-based near-field acoustic holography by means of border-padding. The Journal of the Acoustical Society of America 125.6 (2009), 3844-3854.

[11] R. Blevins: Formulas for natural frequency and mode shape. Van Nostrand Reinhold, New York, 1979.

[12] M. Allen and J. Ginsberg: SIMO extension of the algorithm of mode isolation. Proc. IMAC 22-XXII, 2004.

[13] R. Harder and R. Desmarais: Interpolation using surface splines. Journal of aircraft 9 (1972), 189-191.